Molecular and Cellular Endocrinology 534 (2021) 111367

Contents lists available at ScienceDirect

Molecular and Cellular Endocrinology

journal homepage: www.elsevier.com/locate/mce

# EVI1 overexpression promotes ovarian cancer progression by regulating estrogen signaling

Zixiang Wang [a,b], Yingwei Li [a], Nan Wang [c], Peng Li [b,**], Beihua Kong [b,***], Zhaojian Liu [b,*]

[a] Department of Obstetrics and Gynecology, Qilu Hospital, Cheeloo College of Medicine, Shandong University, Jinan, Shandong, 250012, China
[b] Department of Cell Biology, School of Basic Medical Sciences, Cheeloo College of Medicine, Shandong University, Jinan, 250012, China
[c] Mills Institute for Personalized Cancer Care and Fynn Biotechnologies Ltd, Jinan, Shandong, 250012, China

ARTICLE INFO

*Keywords:*
EVI1
ESR1
Estrogen signaling
Ovarian cancer

ABSTRACT

High-grade serous ovarian cancer (HGSOC) is characterized by TP53 mutation and somatic copy number alterations (SCNAs). Here we show that the oncogenic transcription factor EVI1 (ecotropic viral integration site-1) is amplified and overexpressed up to 30% of 1640 HGSOC cases in The Cancer Genome Atlas (TCGA). Functionally, EVI1 promotes proliferation/invasion *in vitro* and tumor growth of xenograft model *in vivo*. Importantly, we discover that EVI1 regulates estrogen signaling by directly activating ESR1 (estrogen receptor 1) transcription determined by the ChIP and luciferase assay. Interestingly, EVI1 and ESR1 share common regulatory targets as indicated by the analysis of ChIP-Seq data. EVI1 and ESR1 collaborate in the regulation of some estrogen receptor-regulated genes. Furthermore, EVI1 drives tumor aggressiveness partially by regulating estrogen signaling. Estrogen enhances the proliferation, invasion and xenograft growth of ovarian cancer cells. Importantly, estrogen can rescue the inhibition of proliferation, invasion and xenograft growth induced by silencing EVI1. These findings suggest that EVI1 functions as a novel regulator of the estrogen signaling network in ovarian cancer.

## 1. Introduction

Ovarian cancer is the most lethal type of gynecological malignancy. Due to the lack of effective early diagnostic methods, most patients are diagnosed in the late stage. Over 70% of patients relapse with chemotherapy resistance after standard treatment, and the 5-year overall survival rate is only 47% (Siegel et al., 2019). HGSOCs account for 90–95% of cases serous ovarian cancer with high malignancy and a poor prognosis (Labidi-Galy et al., 2017).

HGSOC is characterized by TP53 mutations and somatic copy number alterations (SCNAs). Mutations in TP53 are the earliest known molecular events, with a mutation rate of 96% in HGSOCs. In addition, SCNAs are hallmarks of HGSOC and likely sources of driver alterations in this disease. The most common focal amplifications include CCNE1, MYC and EVI1 (MECOM, MDS and EVI1 complex locus) (Fears et al., 1996). EVI1 is an oncogenic transcription factor involved in the development and progression of several types of malignant tumors including ovarian cancer (Lugthart et al., 2008; Nucifora, 1997; Idel et al., 2020; Mizuguchi et al., 2019; Nanjundan et al., 2007). MECOM is located on chromosome 3q26.2 and encodes multiple transcripts produced by alternative splicing, including MDS-EVI1, EVI1 and EVI1-delta324 (Jazaeri et al., 2010). The fusion protein MDS-EVI1 functions as a tumor suppressor, and EVI1delta324 and EVI1 are considered oncogenes related to a poor prognosis (Lugthart et al., 2008). EVI1 is the main transcript, accounting for the majority of the mRNA and protein produced from MECOM (Nanjundan et al., 2007). EVI1 contains two DNA-binding zinc finger domains, among which the N-terminal zinc finger domain binds to the GATA-like motif and the C-terminal domain binds to the ETS-like motif (Funabiki et al., 1994).

Previous studies indicate that EVI1 participates in several biological processes, including hematopoiesis, apoptosis, and autophagy (Idel et al., 2020; Ma et al., 2019; Ayoub et al., 2018; Pradhan et al., 2011). As

* Corresponding author. Department of Cell Biology, Shandong University School of Medicine, 44 Wenhuaxi Road, Jinan, 250012, Shandong Province, China.
** Corresponding author. Department of Obstetrics and Gynecology, Qilu Hospital, Shandong University, 107 Wenhua Xi Road, Jinan, 250012, Shandong Province, China.
*** Corresponding author. Department of Obstetrics and Gynecology, Qilu Hospital, Shandong University, 107 Wenhua Xi Road, Jinan, 250012, Shandong Province, China.
*E-mail addresses:* peng_li2002@163.com (P. Li), kongbeihua@sdu.edu.cn (B. Kong), liujian9782@sdu.edu.cn (Z. Liu).

https://doi.org/10.1016/j.mce.2021.111367
Received 14 February 2021; Received in revised form 5 June 2021; Accepted 10 June 2021
Available online 17 June 2021

an oncogenic transcription factor, EVI1 regulates hematopoietic stem cell proliferation by modulating GATA-2 and PBX1 expression (Yuasa et al., 2005; Shimabe et al., 2009). EVI1 promotes EGFR transcription in glioblastoma cells (Mizuguchi et al., 2019) and c-Fos expression in NIH3T3 cells (Tanaka et al., 1994). In contrast, EVI1 suppresses the transcriptional activity of Smad3 and represses TGF-beta signaling. Our group previously reported that EVI1 regulates PBK expression by directly targeting the PBK promoter region (Ma et al., 2019). However, a limited number of EVI1 targets have been identified, and the EVI1 regulatory network in ovarian cancer remains unclear (Bard-Chapeau et al., 2012).

In this study, we showed the ubiquitous amplification and overexpression of EVI1 in HGSOC samples, with a copy number amplification frequency as high as 29.9%. EVI1 promoted the invasion and proliferation of ovarian cancer cells both *in vitro* and *in vivo*. Furthermore, EVI1 transcriptionally regulated ESR1 and activated the estrogen signaling network in ovarian cancer. Our data revealed a novel upstream regulatory axis for ESR1 expression in ovarian cancer.

## 2. Materials and methods

### 2.1. Patients and tissue preparation

HGSOC specimens and fallopian tube tissues used to detect expression were collected from the Department of Obstetrics and Gynecology, Qilu Hospital, Shandong University from April 2009 to July 2015. The HGSOC samples were obtained from patients with primary ovarian cancer who had not undergo a previous surgery or chemotherapy. In addition, fallopian tube tissues were obtained from patients who underwent total hysterectomy and bilateral salpingo-oophorectomy for uterine diseases or benign neoplastic adnexal pathological changes. The study was approved by the Ethics Committee of Shandong University, and all patients provided written informed consent. Fresh tissue samples were collected within 2 h of surgery. Fresh tissues were sliced to 5 $mm^3$ and immersed in 10 vol of RNALater (Ambion, Austin, TX). Then, the tissue samples were stored at -80 °C. All patients provided informed consent. Ethical approval was granted by the Ethics Committee of Shandong University (SDULCLL2019-1-09).

### 2.2. Bioinformatics analysis

ChIP-Seq datasets including peak information for EVI1 (GSE25210), ESR1 (GSE116005) and H3K27ac (GSE101408) in bed or narrowpeak format were obtained from the Gene Expression Omnibus (GEO) database. Gene expression profiles of ovarian cancer cells were obtained from GEO accessions GSE25213 and GSE115481. All the datasets were mapped to the human genome (version hg19). An R/Bioconductor software package limma was used for differential expression analysis (Ritchie et al., 2015). Overlap peaks were calculated with BEDTools (Quinlan and Hall, 2010). These regions were visualized with Integrative Genomics Viewer (IGV) (Robinson et al., 2017) and placed in genomic context with the ChIPseeker package (Yu et al., 2015). The copy number and mRNA expression information in the TCGA and GTEx databases were viewed and downloaded with UCSC Xena (Goldman et al., 2020) and GEPIA2 (Tang et al., 2019). Analyses of function enrichment of differentially expressed genes were conducted using PANTHER (Mi et al., 2020), Gene Ontology (The, 2019), GSEA (Subramanian et al., 2005), and MSigDB (Subramanian et al., 2005) and plotted using ImageGP (http://www.ehbio.com/ImageGP/). Protein-protein interaction (PPI) networks of estrogen-responsive genes were constructed using the STRING database (http://stringdb.org/). R/Bioconductor 3.6.3 was used for plotting. GraphPad Prism 8 was used for the Pearson correlation analysis, and Kaplan-Meier plots were tested using log-rank tests.

### 2.3. Cell culture and treatment

A2780, HEY, and SKOV3 cell lines were obtained from Jian-Jun Wei. OV90 cell line was purchased from American Type Culture Collection. A2780, HEY, and OV90 cells were cultured in Dulbecco's Modified Eagle's Medium (DMEM) (Gibco, Invitrogen). SKOV3 cells were cultured in McCoy's 5A medium. All culture media contained 10% fetal bovine serum (FBS) (Gibco, Grand Island, NY, USA). The cells were cultured at 37 °C in a humidified incubator containing 5% CO2.

### 2.4. RNA isolation and qPCR

Total RNA was extracted from cultured cells or fresh tissues with a Cell Total RNA Isolation Kit (Foregene, Chengdu, China) according to the manufacturer's instructions. Total RNA was reverse transcribed into cDNAs using HiScript II Q RT SuperMix for qPCR (Vazyme, China). qPCR was performed to detect mRNA expression using the Bio-Rad CFX96 real-time PCR detection system. Primer information is listed in Supplementary Table S2.

### 2.5. Western blot

The samples were lysed on ice in RIPA buffer (Beyotime Institute of Biotechnology, China) and the protein concentration was determined using the BCA assay (Beyotime Institute of Biotechnology, China). SDS-PAGE and electrophoresis were used to separate protein samples. The membrane was blocked with 5% skim milk before an overnight incubation with primary antibodies at 4 °C. Primary antibodies included anti-EVI1 (Abcam, 124934), anti-E-cadherin (CST, 3995), anti-N-cadherin (CST, 13116), anti-vimentin (CST, 5741), anti-Snail (CST, 3879), anti-Slug (CST, 9585), anti-ZO1 (Abclonal, A0659), anti-ESR1 (Abcam, 32063), and anti-NOV (Abcam, 191425). All the antibodies were diluted as 1:1000 except anti-ESR1 was diluted as 1:500. Horseradish peroxidase-conjugated secondary antibodies and an ECL system (GE Healthcare, Little Chalfont, Buckinghamshire, UK) were used to detect specific proteins.

### 2.6. Plasmids, siRNAs, and small molecules

The EVI1 (MECOM, NM_001164000) overexpression plasmid pCMV-Ubi-MCS-3FLAG-SV40-EGFP-IRES-puromycin (pCMV-FLAG-EVI1) and the control plasmid (pCMV-FLAG) were constructed by GeneChem (Shanghai, China). The siRNAs targeting ESR1 were prepared by GenePharma, China, and the sequences of siRNA duplexes were obtained from a previous study (Zhang et al., 2005) and are listed in Supplementary Table S1. Plasmids and siRNAs were transiently transfected into cells with jetPRIME transfection reagent (PolyPlus, Illkirch, France), according to the manufacturer's instructions. RNA or protein was extracted after 48 or 72 h of transfection separately. 100 nM β-Estradiol (Sigma, E2758), 5 μM fulvestrant (Targetmol, T2146) were added to ovarian cancer cells 48 h before the rescue experiment.

### 2.7. Lentiviral vector construction and infection

The shRNA duplexes targeting EVI1 were constructed with the sequences indicated in Supplementary Table S1. After annealing, the fragment was cloned into the pLKO.1-puro vector. pCMV-FLAG-EVI1 was constructed by GeneChem as described above. These lentivirus plasmids, along with pMD2.G and psPAX2 were cotransfected into HEK293T cells for lentivirus production. Cells were infected with lentivirus for 48 h and selected with 2 μg/ml puromycin (Merck Millipore, Billerica, MA, USA) for 2 weeks to acquire cell lines with stable expression. The morphological-functional characteristics of control and experimental group were checked under the same passage number.

### 2.8. Cell proliferation assay

An EdU cell proliferation assay was performed using an EdU Kit (RiboBio, Guangzhou, China) according to the manufacturer's instructions. Briefly, cells were seeded on glass coverslips in 24-well plates at densities of 4-6 $\times$ $10^4$ cells per well before the incubation with cell culture medium containing EdU for 20-30 min. The cells were fixed and stained with Apollo fluorescent dye and Hoechst 33342. The MTT assay was also used to examine cell proliferation. Cells were seeded in 96-well plates in triplicate wells at densities of 1 $\times$ $10^3$ cells per well. Cell proliferation was monitored for the next 5 days. After culture for the designated time, 10 μl of MTT reagent (5 mg/ml) was added to each well and incubated for 4 h at 37 °C. The supernatant was discarded, and 100 μl of dimethyl sulfoxide (DMSO) was added to each well. Then, the absorbance was measured at 570 nm using a microplate reader (Bio-Rad, Hercules, CA, USA).

### 2.9. Colony formation assay

Cells were seeded in a six-well plate (1000-2000 cells per well) and cultured for 1-2 weeks. Colonies were fixed with methanol, stained with 0.1% crystal violet, and the number of colonies was counted. All experiments were repeated at least three times.

### 2.10. Immunohistochemistry

Formalin-fixed and paraffin-embedded tissues were sectioned at 4 μm. Then, tissue sections were deparaffinized in xylene and rehydrated with a graded series of ethanol solutions. Antigen retrieval was performed in ethylenediaminetetraacetic acid (EDTA) and heated in a microwave. Nonspecific antigens were blocked with 1.5% normal goat serum. Sections were incubated with a primary antibody against Ki-67 (1:200 dilution, CST, 9129S), ESR1 (1:200 dilution, abcam, 32063), EVI1 (1:50 dilution, Santa Cruz, sc-515456) overnight at 4 °C. Then, sections were incubated with secondary antibody and stained with diaminobenzidine.

### 2.11. Matrigel invasion assay

Matrigel invasion assays were performed in Matrigel-coated chambers with 8 μm pore sizes (BD Falcon, Bedford, MA, USA) in 24-well plates. Matrigel was diluted 1:10 with FBS-free DMEM. A total of 1.0-1.5 $\times$ $10^5$ cells was plated into the upper chambers in 200 μl of medium lacking FBS, and the lower chambers were filled with 700 μl of culture media containing 30% FBS as a chemoattractant. The chambers were incubated at 37 °C for 4-48 h, depending on the different cell lines. Successfully invaded cells were fixed with methanol and stained with 0.1% crystal violet for 20 min.

### 2.12. Chromatin immunoprecipitation assay

ChIP (chromatin immunoprecipitation) assays were conducted using an EZ-Magna ChIP A/G chromatin immunoprecipitation kit (Merck KGaA, Darmstadt, Germany) according to the manufacturer's instructions. DMSO, fulvestrant (5 μM), and estrogen (100 nM) were incubated with SKOV3 cells 72 h before harvest. About 1.0 $\times$ $10^7$ SKOV3 cells per sample were cross-linked and lysed in lysis buffer, and DNA was sheared to ~200-500 bp fragments by sonication. Cell lysates were incubated with an EVI1 antibody (Santa Cruz, sc-515456) and magnetic beads overnight at 4 °C with rotation. Rabbit IgG was used as the negative control. The purified DNA was subjected to RT-qPCR and PCR, and the primer sequences are listed in Supplementary Table S2.

### 2.13. Luciferase reporter assay

The Dual-Glo Luciferase Assay System (Promega) was used for the luciferase reporter assay. For the promoter reporter assay, PGL4.26 plasmids containing the ESR1 promoter and its mutants were cotransfected with the EVI1 overexpression plasmid into A2780 cells. Deletion mutants were constructed with the QuikChange mutagenesis method, and primers used for plasmid construction are listed in Supplementary Table S3. 48 h later, the cells were lysed, and the intracellular luciferase activity was measured according to the manufacturer's instructions.

### 2.14. CRISPR/Cas9 genome editing

CRISPR/Cas9 System was used to edit the ETS-like motif of ESR1 promoter according to the previously reported method (Ran et al., 2013). sgRNA was designed with CRISPick (https://portals.broadinstitute.org/gppx/crispick/public). Three sgRNAs near or inside the ETS-like motif were selected and the primers were listed in Supplementary Table S4. Then the annealed primers were cloned into the LentiCRISPRv2 plasmid (Addgene, #52961). The ssODN template used was absent of the ETS-like motif. The constructed LentiCRISPRv2 plasmid was cotransfected with ssODN (10 μM) into A2780 cells with jetPRIME transfection reagent, according to the manufacturer's instructions. Incubate the mixture for 48 h and then puromycin selection was applied for 72 h. Cells were culture for 1 week and then used for genotyping.

### 2.15. Nude mouse xenograft model

Female BALB/c-nude mice (6-8 weeks old) were randomly divided into two groups (4 mice per group) and injected subcutaneously with EVI1 knockdown and control HEY cells as previously described (Wang et al., 2017a). The volume and weight of tumors were monitored for the next 2 weeks. In the rescue experiment *in vivo*, mice were randomly divided into four groups (6 mice per group) to receive either vehicle (DMSO plus phosphate-buffered saline every three days) or estradiol benzoate (100 mg/kg body weight every three days). Estradiol benzoate (Targetmol, T0384) and vehicle were administered intramuscularly. 17 days after tumor cell inoculation, the mice were sacrificed and the tumors weight and volume were measured. The Shandong University Animal Ethics Research Board approved all animal procedures (SDULCLL2019-2-08).

### 2.16. Statistical analysis

GraphPad Prism 8 and the R package (v.3.6.3, http://www.r-project.org/) were used for statistical analyses. Student's t-test and one-way analysis of variance (ANOVA) were used to determine significant differences. The results are presented as the means ± S.D. of three independent experiments. A total of 10,000 randomly selected genes were used to compute the empirical p value of the overlapping genes. Statistical significance was considered as *$p < 0.05$, **$p < 0.01$, ***$p < 0.001$, and ****$p < 0.0001$.

## 3. Results

### 3.1. EVI1 is ubiquitously amplified and overexpressed in HGSOCs

Somatic copy number alterations (SCNAs) play an important role in carcinogenesis. We analyzed SCNAs in 1640 samples using three TCGA HGSOC cohorts. Importantly, HGSOC samples had a high SCNA frequency, and sixteen genes had a frequency greater than 20% across all samples. We chose EVI1 (MECOM), which was the third most amplified gene (29.9%) in HGSOCs, for further investigation (Fig. 1A and S1A). In addition, EVI1 was highly amplified in lung squamous carcinoma and ovarian cancer among all cancers in TCGA datasets (Fig. 1B). The copy number detected in HGSOC was higher than that in blood and normal ovarian tissue (Fig. S1B). We subsequently analyzed the correlation between amplification and expression, and these parameters were

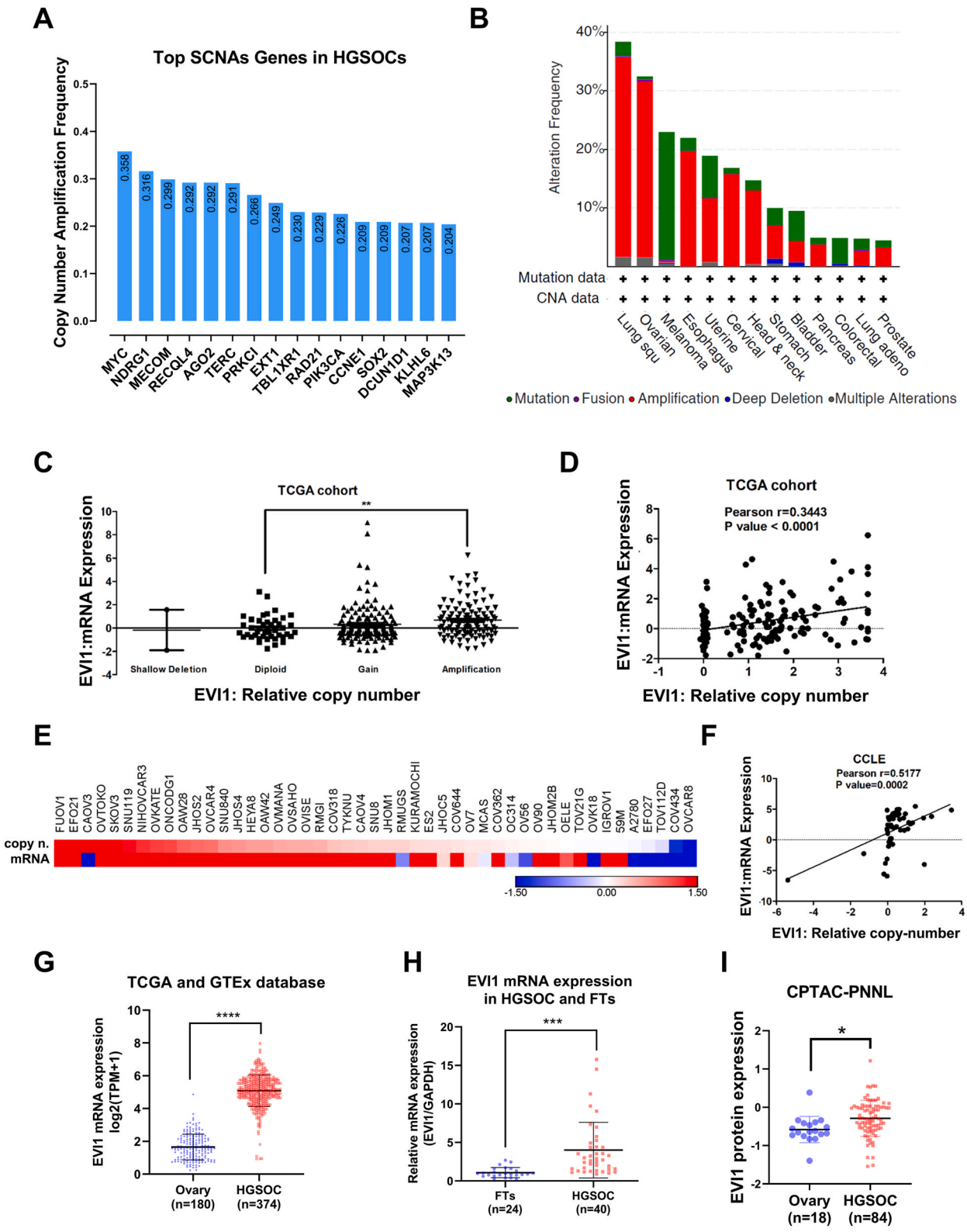


**Fig. 1.** Ubiquitous amplification and overexpression of EVI1 in HGSOC tissues. (A) 16 genes with copy number amplification frequencies greater than 20% in HGSOC samples from TCGA databases were identified. (B) The pan-cancer analysis revealed genetic mutations and copy number alterations in EVI1 in different cancers from cBioPortal. (C) Relative expression of the EVI1 mRNA in copy number shallow deletion, diploid, gain, and amplification groups from TCGA cohorts was analyzed. (D) The correlation between the EVI1 copy number and mRNA expression was calculated in TCGA cohorts ($r = 0.3443$, $p < 0.0001$). (E and F) The correlation between the EVI1 copy number and mRNA expression was calculated in the CCLE cohort ($r = 0.5177$, $p = 0.0002$). (G) EVI1 mRNA expression levels were analyzed in 374 TCGA HGSOC samples and 180 normal ovarian tissue samples. (H) EVI1 mRNA expression was measured in 40 HGSOC tissues and 24 fallopian tube tissues (FTs) using qPCR. (I) EVI1 protein expression was analyzed in 84 HGSOC tissues and 18 normal ovary tissues (FTs, $n = 24$) in CPTAC-PNNL datasets. Data are presented as means ± S.D. *$p < 0.05$, **$p < 0.01$, ***$p < 0.001$, and ****$p < 0.0001$.

positively correlated, indicating that both the mRNA and protein levels of EVI1 in amplification samples were higher than in the diploid group ($r = 0.3443$, $p < 0.0001$) (Fig. 1C-D and S1C-D). The correlation between the copy number and mRNA expression was further confirmed in ovarian cancer cell lines using the Cancer Cell Line Encyclopedia (CCLE) cohort ($r = 0.5177$, $p = 0.0002$) (Fig. 1E-F). We further analyzed EVI1 expression in HGSOC and normal tissues using TCGA and GTEx data. EVI1 was commonly overexpressed in HGSOC tissues compared to normal tissues (Fig. 1G and S1E). Moreover, we validated EVI1 expression in our cohort using qPCR and detected much higher EVI1 expression in HGSOCs than in normal FTs (Fig. 1H). The protein level of EVI1 was also upregulated in HGSOC samples based on CPTAC-PNNL data (Fig. 1I). Similarly, EVI1 expression levels were commonly upregulated in ovarian cancer cell lines compared to the immortalized fallopian tube epithelial cell line FTE187 (Fig. S1F-G). Based on these data, EVI1 is frequently amplified and overexpressed in HGSOC.

### 3.2. EVI1 promotes migration, invasion and induces epithelial mesenchymal transition (EMT) of ovarian cancer cells in vitro

We first conducted a Gene Ontology (GO) analysis of the transcriptome in SKOV3 cells with EVI1 knockdown (GSE25213) to determine whether EVI1 was involved in the initiation and progression of ovarian cancer. Interestingly, genes associated with cell migration and cell adhesion were significantly overrepresented among the genes regulated by EVI1 (Fig. 2A). Additionally, the gene set enrichment analysis (GSEA) revealed that the EMT pathway was highly enriched among EVI1-regulated genes (Fig. 2B). Thus, EVI1 might be involved in the invasion and EMT of ovarian cancer cells. Interestingly, EVI1 overexpression resulted in a more spindle-like morphology of A2780 cells after establishment of stable transfected cell lines (Fig. 2C). Then we performed wound healing assay and found overexpression of EVI1 significantly enhanced the migration capacity of A2780 cells, whereas knockdown of EVI1 decreased the migration of SKOV3 and HEY cells (Fig. 2D). Consistent with these findings, the results of the transwell invasion assays also showed that overexpression of EVI1 in A2780 cells significantly increased invasion, while EVI1 knockdown produced the opposite effect on HEY, SKOV3 cells (Fig. 2E and S2A). We further measured the expression level of EMT-related markers using western blot. As expected, ectopic expression of EVI1 led to the upregulated expression of mesenchymal markers and reduced levels of epithelial markers in A2780 cells. In contrast, EVI1 knockdown resulted in decreased expression of mesenchymal markers and higher expression of epithelial markers in SKOV3 cells (Fig. 2F). Therefore, EVI1 promotes migration and invasion and induces the EMT in ovarian cancer cells.

### 3.3. EVI1 increases ovarian cancer proliferation in vitro and xenograft tumor growth in vivo

An analysis of enriched GO terms in the transcriptome of SKOV3 cells with EVI1 knockdown (GSE25213) also revealed the enrichment of genes involved in epithelial cell proliferation. We then conducted an EdU (5-ethynyl-2′-deoxyuridine) assay and found that EVI1 overexpression significantly increased the number of EdU-positive cells, while knockdown of EVI1 decreased the ratio of EdU-positive cells compared with the control group (Fig. 3A and S2B). Consistent with the EdU data, ectopic expression of EVI1 also significantly increased the proliferation of ovarian cancer cells, as measured by growth curve and clonogenic assays (Fig. 3B-C and S2C-D). We further confirmed the function of EVI1 in tumor growth by establishing subcutaneous xenograft model using HEY cells with EVI1 knockdown or control cells ($n = 4$). Importantly, EVI1 knockdown significantly reduced the tumor volume and weight (Fig. 3D-G). Additionally, the number of Ki-67-positive cells was significantly decreased in tumors with EVI1 depletion (Fig. 3H). Based on these results, EVI1 facilitates ovarian cancer cell proliferation *in vitro* and xenograft tumor growth *in vivo*.

### 3.4. EVI1 positively regulates ESR1 expression in ovarian cancer cells

We first analyzed ChIP-Seq data in SKOV3 cells to explore EVI1-regulated targets and signaling pathways involved in the regulation of ovarian cancer malignancy. Notably, 4202 of 39470 peaks were located within the promoter region (Fig. 4A). Next, we analyzed the transcriptome analysis of SKOV3 cells with EVI1 knockdown using a microarray. A volcano plot showed 1169 upregulated and 1444 downregulated genes in SKOV3 cells with EVI1 knockdown (Fig. 4B). The combination of ChIP-Seq and transcriptome analyses revealed 396 predicted EVI1 targets (Fig. 4C and Supplementary Table S6). Among these potential targets, 131 were upregulated and 265 were downregulated, indicating that EVI1 positively or negatively regulates downstream targets (Fig. 4D). Notably, estrogen receptor binding ranked as the most enriched term based on a functional enrichment analysis of 396 candidate genes (Fig. 4E), EVI1 and ESR1 transcriptome data (Fig. S3A-C). We further validated potential EVI1 targets, including ESR1, NOV, HMGA1, GATA2 using qPCR. As expected, ESR1, NOV, HMGA1, and GATA2 were significantly downregulated in SKOV3 cells upon EVI1 depletion (Fig. 4F-G). We further validated ESR1 and NOV protein expression using western blot and detected increased levels of these proteins after the overexpression of EVI1 in A2780 cells, while knockdown of EVI1 decreased their levels in HEY and SKOV3 cells (Fig. 4H-I). These findings suggest that ESR1 is a putative EVI1 target in ovarian cancer.

### 3.5. EVI1 directly binds the ESR1 promoter and induces its expression

We sought to determine whether EVI1 was a direct transcriptional activator of ESR1 in ovarian cancer. The MACS2 analysis showed that EVI1 was enriched at the transcription start site (TSS) region of ESR1 (Fig. 5A). Subsequently, we conducted a ChIP assay with an anti-EVI1 antibody to detect endogenous EVI1 in SKOV3 cells. ChIP-PCR data revealed that EVI1 significantly pulled down immunoprecipitated DNA harboring putative EVI1 binding sites compared with the IgG antibody. Importantly, estrogen but not fulvestrant (estrogen receptor antagonist) could increase the binding of EVI1 to ESR1 promoter (Fig. 5C–D). PGL4.26 plasmids carrying the ESR1 promoter region with wild-type or mutant EVI1 binding sites (−1287 to 279 related to TSS) were constructed (Supplementary Table S5). A luciferase assay was then performed in A2780 cells, and the overexpression of EVI1 increased the luciferase activity of ESR1 promoter reporters carrying wild-type EVI1 binding sites, but the luciferase activity of ESR1 promoter reporters carrying mutant EVI1 binding sites was lower than the wild-type reporters after EVI1 overexpression (Fig. 5E). CRISPR/Cas9 system was further applied to edit EVI1 binding site on ESR1 promoter and ESR1 mRNA was measure by qPCR with EVI1 overexpression. As a result, EVI1 overexpression failed to increase ESR1 expression in ESR1 promoter edited cells compared to wildtype cells (Fig. 5F). Importantly, the analysis of CCLE and TCGA data revealed that the expression level of EVI1 was correlated with ESR1 expression in HGSOCs (Fig. 5G-H), which was validated with our clinical samples ($n = 62$) (Fig. 5I). Immunohistochemistry staining further showed that both EVI1 and ESR1 was highly expressed in HGSOCs (Fig. 5J). Furthermore, ESR1 expression was significantly decreased in xenograft tumors with EVI1 depletion (Fig. 5K). Not surprisingly, ESR1 was upregulated in HGSOC samples ($n = 374$) compared to control ovarian tissues, and high levels of ESR1 indicated a poor prognosis ($n = 180$) (Fig. S3D-F). These data strongly indicate that EVI1 directly binds the ESR1 promoter and induces its expression.

### 3.6. EVI1 coregulates the ESR1 transcription program and reinforces estrogen signaling

We first analyzed whether EVI1 and ESR1 share common regulatory targets to obtain a better understanding of the effect of EVI1 on ESR1

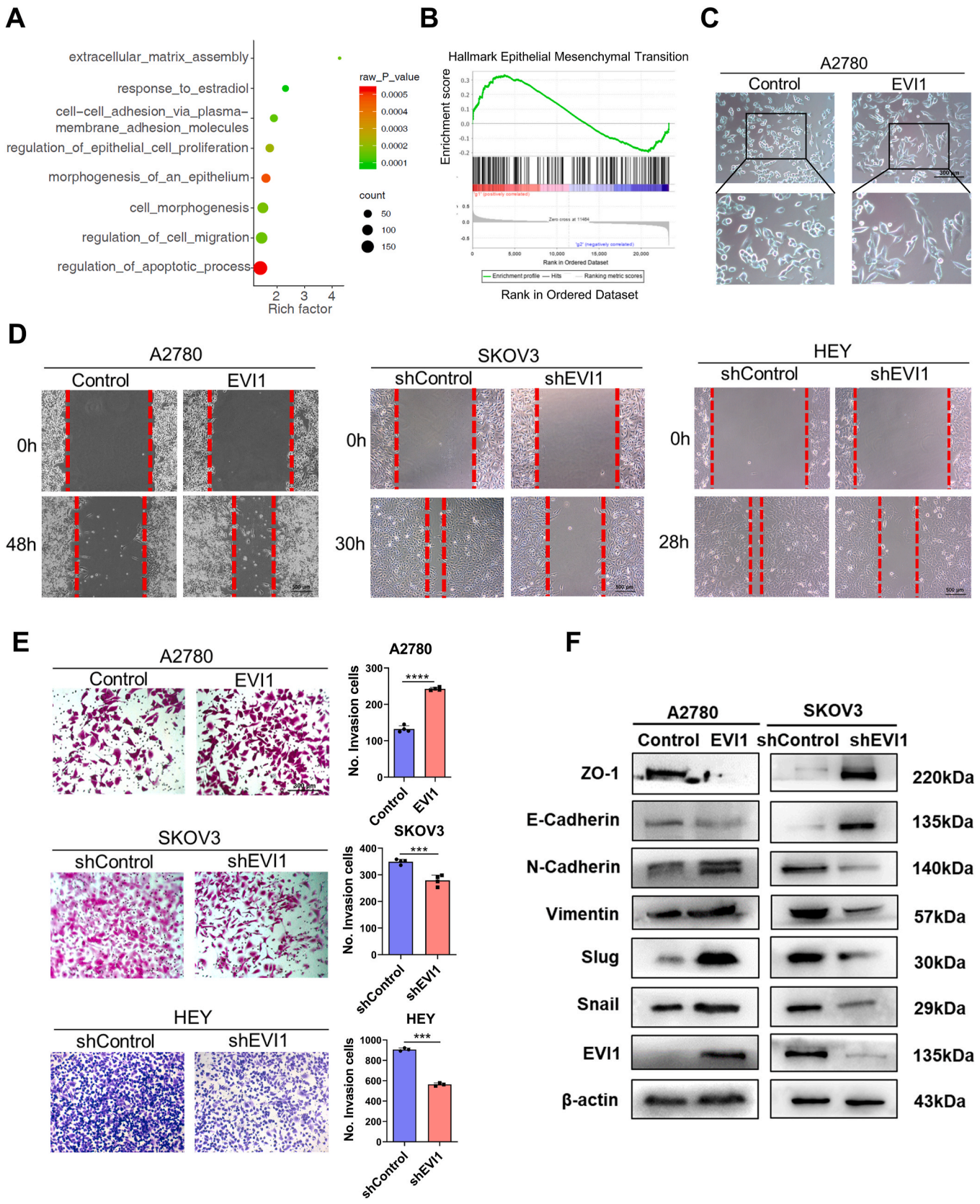


**Fig. 2.** EVI1 promotes cell invasion and metastasis and induces the EMT in ovarian cancer cells. (A) Gene Ontology (GO) analysis of 2613 differentially expressed genes in transcriptome data. (B) The GSEA showed that the EMT pathway was enriched among differentially expressed genes in SKOV3 cells with EVI1 knockdown (GSE25213) (enrichment score = 0.33, $p < 0.001$). (C) Morphological changes in A2780 cells overexpressing EVI1 were observed under a microscope. Both A2780-NC and A2780-EVI1 cells were passage no.5 from the time when the stable transfection cell lines were constructed. (D-E) Wound healing and matrigel invasion assays were conducted in ovarian cancer cell lines with EVI1 overexpression (A2780) or knockdown (SKOV3, HEY). (F) Western blot analysis of EMT-related markers in ovarian cancer cells with EVI1 overexpression or knockdown. Data are presented as means ± S.D. *$p < 0.05$, **$p < 0.01$, ***$p < 0.001$, and ****$p < 0.0001$.

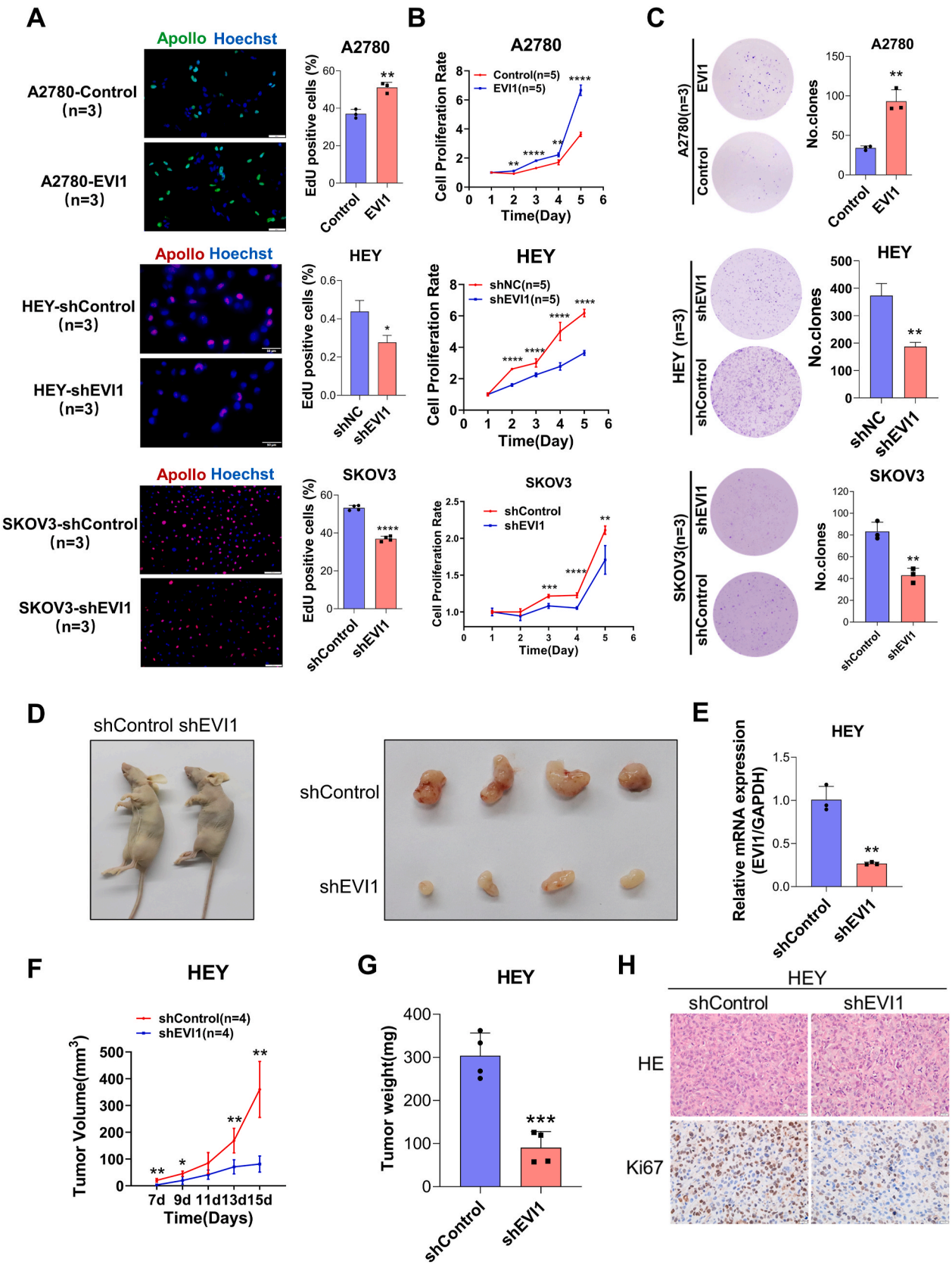


**Fig. 3.** EVI1 increases ovarian cancer cell proliferation and the growth of xenograft tumors. (A-C) The effect of EVI1 on the proliferation of ovarian cancer cells was examined by performing (A) EdU, (B) growth curve and (C) clonogenic assays of ovarian cancer cells with EVI1 overexpression (A2780) or knockdown (HEY, SKOV3) compared to the corresponding controls. (D) Representative images of xenograft tumors of HEY cells with EVI1 knockdown compared to the control cells. (E) EVI1 mRNA expression in xenograft tumors. (F-G) Tumor volume and weight in HEY cell xenograft tumors were analyzed. (H) Representative images of HE staining and IHC staining for Ki-67 in HEY cell xenograft tumors. Data are presented as means ± S.D. *p < 0.05, **p < 0.01, ***p < 0.001, and ****p < 0.0001.

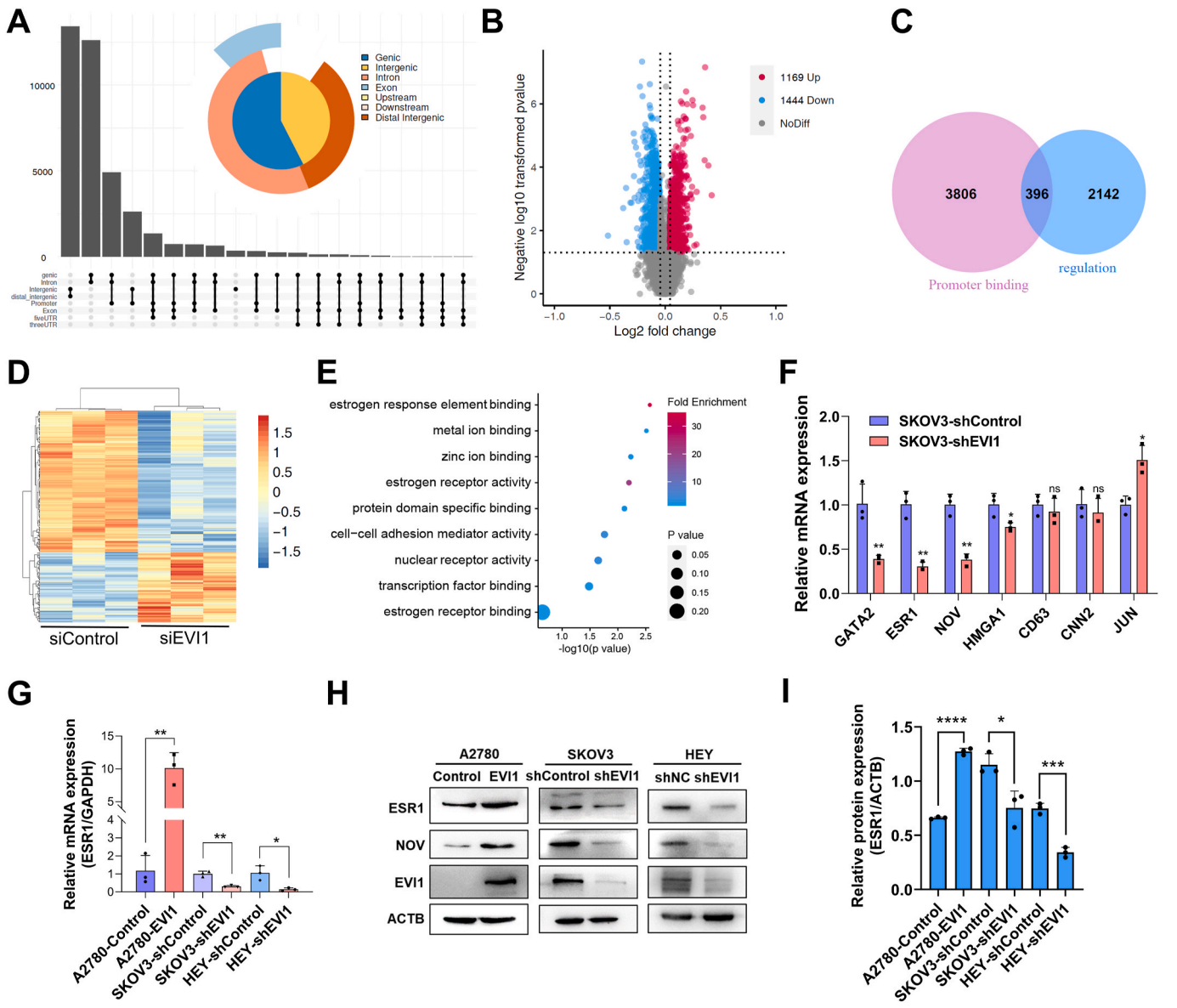


**Fig. 4.** EVI1 positively regulates ESR1 expression in ovarian cancer cells. (A) The EVI1 ChIP-Seq peak (38649 peaks) distribution pattern was analyzed in SKOV3 cells. A total of 4529 peaks were located at the promoter region of downstream genes. (B) Volcano plot of differentially expressed genes in the transcriptome of SKOV3 cells after EVI1 knockdown. 1169 genes were upregulated, and 1444 genes were downregulated ($p < 0.05$, $|FC| > 1.03$). (C) Venn diagram of integrated ChIP-Seq and transcriptome data showing 396 predicted EVI1 targets. (D) Heatmap of mRNA expression of the EVI1 target genes in SKOV3 cells. (E) Enrichment analysis of the GO terms of the 396 target genes. (F) Validation of predicted targets at the mRNA level in SKOV3 cell lines with EVI1 knockdown. (G) qPCR was applied to validate the relative expression of ESR1 in A2780, SKOV3, and HEY cell lines with EVI1 overexpression and knockdown. (H-I) EVI1, ESR1, NOV, and ACTB protein expression was determined with western blot in A2780, SKOV3, and HEY cell lines with EVI1 overexpression and knockdown. Blots were quantitated for ESR1 protein with ImageJ. Data are presented as means ± S.D. *$p < 0.05$, **$p < 0.01$, ***$p < 0.001$, and ****$p < 0.0001$.

activation in ovarian cancer. By comparing the EVI1 ChIP-Seq data and ESR1 ChIP-Seq from SKOV3 ovarian cancer cells, we identified 10541 peaks (26.7% of EVI1 peaks) that were shared by EVI1 and ESR1 (Fig. 6A). Approximately 21.9% of the overlapping peaks (2308 peaks) were located in the promoter region (-3 kb to +3 kb of TSS) (Fig. 6B). However, the majority of EVI1 and ESR1 binding peaks did not overlap with each other, indicating that these proteins can function independently. We next analyzed the estrogen early response genes from MSigDB (Liberzon et al., 2015), and EVI1 bound to 50 of 200 promoter regions of estrogen early response genes. This result represents an enrichment of 2.28-fold (p value = $3.33e^{-10}$) over the expected reference ratio of 0.95% calculated with 10000 random genes. The subset of the 50 genes was clustered with a normalized enrichment factor of 1.32 by GSEA (FDR 8%, FWER p-value < 0.05) (Fig. 6C). Several classical ESR1 target genes, including GREB1, RARA, MREG, FRK, TGM2, KLF4, and KRT19 (Ross-Innes et al., 2012), were identified in the subset with overlapping binding sites for both EVI1 and ESR1. The overlapping peaks were mostly located near the TSS (-3 kb to +3 kb) in the promoter regions and transcriptionally active regions, based on colocalization with H3K27ac (Fig. 6D-E). A transcriptome expression heatmap of the subset of 50 genes is shown (Fig. 6F). Moreover, we validated 6 ESR1 target genes using qPCR and found that GREB1, RARA, MREG, FRK, TGM2, and KRT19 were significantly upregulated in A2780 cells overexpressing EVI1. Interestingly, inhibition ESR1 activity by fulvestrant could attenuate EVI1 induced upregulation of estrogen receptor-regulated genes (four of six) including GREB and RARA (Fig. 6G). These data suggest that EVI1 and ESR1 could collaborate in the regulation of some estrogen receptor-regulated genes.

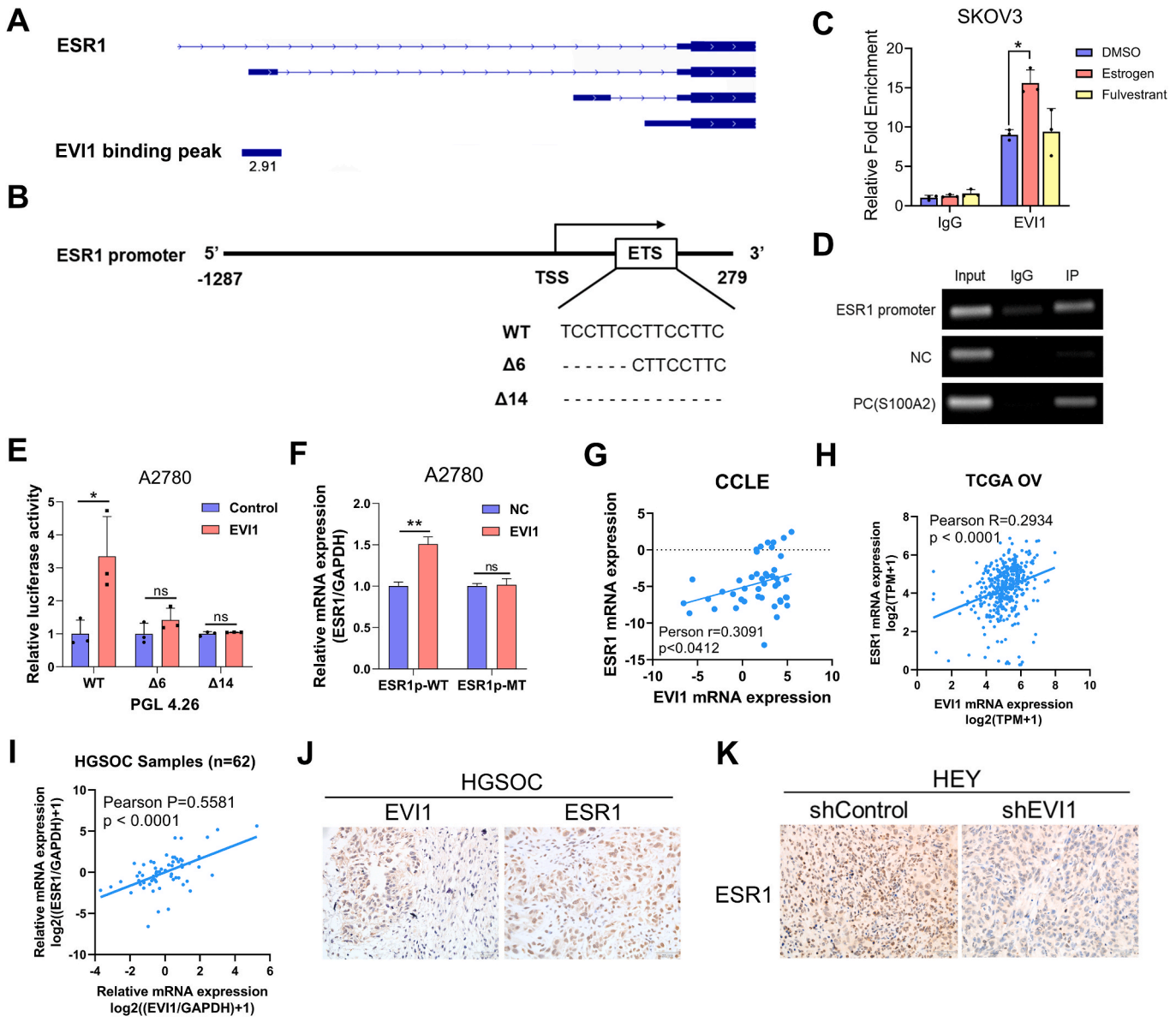


**Fig. 5.** EVI1 directly binds the ESR1 promoter and induces its expression. (A) The EVI1 binding peak at the promoter of ESR1 was visualized with Integrative Genomics Viewer (IGV) in ChIP-Seq data from the GEO database (GSE25210). (B) Potential binding site for EVI1 in the promoter region of ESR1 (GSE116005). The ETS-like motif was located 63 bp after the TSS and contains three clustered TCCTTC binding sites. (C) ChIP-qPCR of the endogenous EVI1 protein bound to the promoter region of ESR1 in SKOV3 cells. Estrogen (100 nM) or fulvestrant (5 μM) was added 72 h before harvest. (D) ChIP-PCR of ESR1 promoter bound by EVI1. A random selected intergenic region on chromosome 10 was used as NC (negative control) and the promoter region of S100A2 was used as PC (positive control). (E) Luciferase activity was measured in ovarian cancer A2780 cells cotransfected with the EVI1 overexpression plasmid and pGL4.26 plasmid containing the ESR1 promoter region (wild type and 6 bp and 14 bp deletion mutants). (F) mRNA expression of ESR1 after overexpression EVI1 in WT (wild type) and MT (mutant type) A2780 cells. Mutant type A2780 acquired a perturbation inside ETS-like motif of ESR1 promoter edited by CRISPR/Cas9 system. (G–H) The correlation between ESR1 and EVI1 mRNA expression was calculated in CCLE and TCGA cohorts (Pearson $R = 0.2934$, $p < 0.0001$). (I) The correlation between ESR1 and EVI1 mRNA expression was calculated in 62 HGSOC samples. Relative mRNA expression was determined with qPCR (Pearson $R = 0.5581$, $p < 0.0001$). (J) IHC (immunohistochemistry) staining was performed in HGSOC samples ($n = 62$). (K) IHC stain of ESR1 in EVI1 knockdown HEY cells of the mouse xenograft model. Data are presented as means ± S.D. *$p < 0.05$, **$p < 0.01$, ***$p < 0.001$, and ****$p < 0.0001$.

### *3.7. EVI1-induced ESR1 signaling activation is required for ovarian cancer progression*

To investigate the functional consequent of EVI1 induction of ESR1 in ovarian cancer progression, we treated EVI1 silenced SKOV3 cells with estrogen. Importantly, estrogen enhanced the proliferation, invasion ability of ovarian cancer cells and estrogen effectively rescued the inhibition of proliferation, invasion induced by silencing EVI1 in SKOV3 cells (Fig. 7A-D). Similarly, estrogen treatment also reversed the inhibitor effect upon EVI1 knockdown in HEY cells (Fig. S4A-B). Importantly, in a xenograft model of HEY cells, estrogen could contribute to tumorigenesis and reverse the inhibition of xenograft growth induced by EVI1 silencing (Fig. 7E-G). On the other hand, we treated EVI1 overexpressed A2780 cells with fulvestrant. We next measured ESR1 level by western blot and found fulvestrant reversed the increased ESR1 expression induced by EVI1 (Fig. 7H). Functionally, fulvestrant significantly inhibited proliferation and invasion ability caused by forced EVI1 expression (Fig. 7I-K). These data indicate that EVI1 promotes malignant behaviors of ovarian cancer by activating ESR1 signaling.

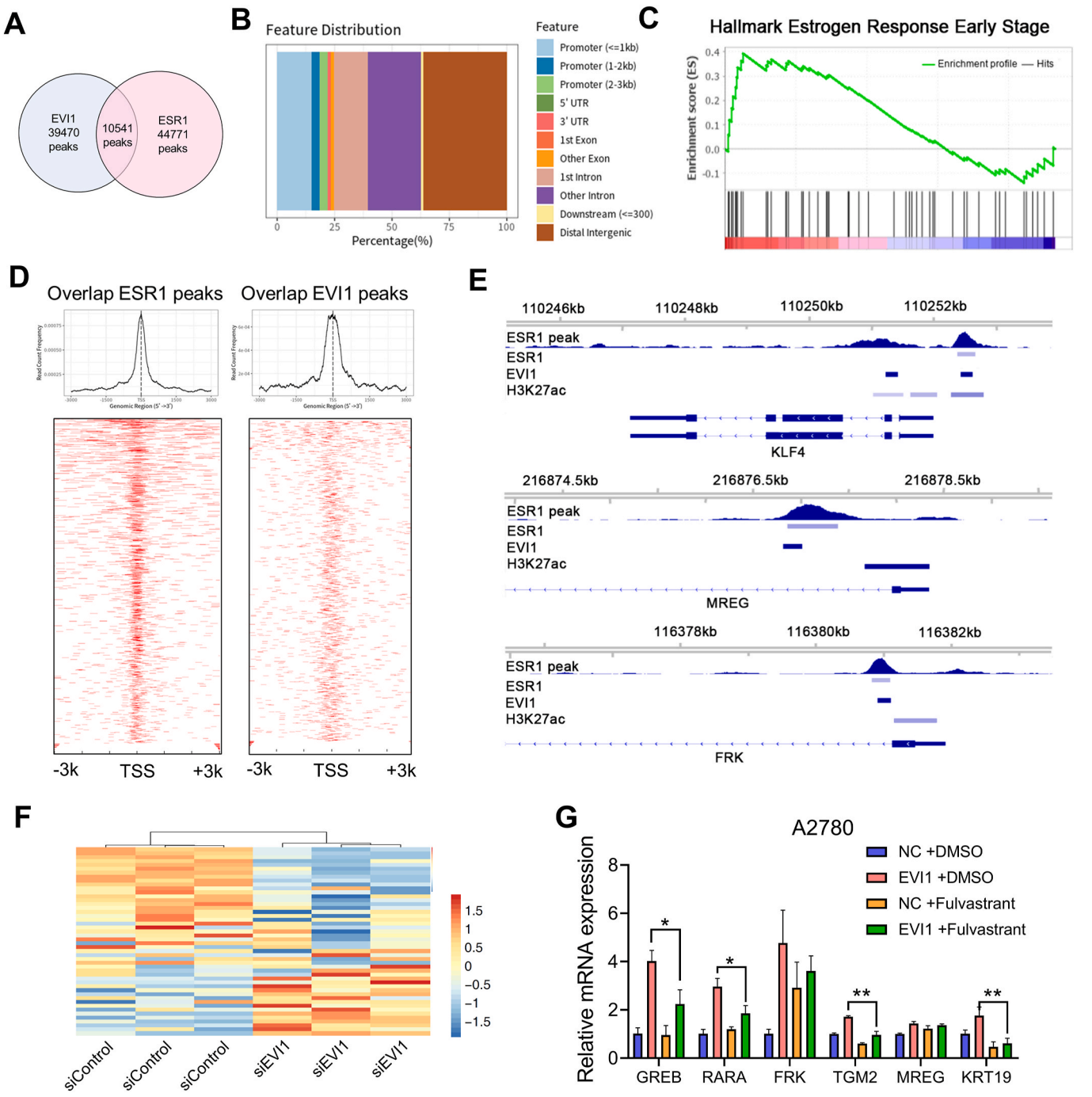


**Fig. 6.** EVI1 coregulates the ESR1 transcription program and reinforces estrogen signaling. (A) Overlapping peaks between EVI1 and ESR1 ChIP-Seq data identified by MACS2 (Model-based Analysis of ChIP-Seq) (Feng et al., 2012). (B) Overlapping peaks located at specific genomic positions, including the promoter region (~23%), were identified. (C) GSEA showed that estrogen early response hallmarks were enriched in the transcriptome of EVI1 knockdown SKOV3 cells (normalized enrichment score (NES) = 1.32, FWER p-value = 0.04). (D) Heatmap showing overlapping peak signals around the TSS (-3 kb to +3 kb) of EVI1 and ESR1 ChIP-Seq data. (E) Colocalization of EVI1, ESR1 and H3K27ac peaks at the promoter regions of typical estrogen-responsive genes, including KLF4, MREG, and FRK. (F) Heatmap showing the expression of 50 estrogen early response genes in the transcriptome of EVI1 knockdown SKOV3 cells (GSE25213). (G) The relative mRNA expression of the coregulated targets between ESR1 and EVI1 was determined using qPCR, including GREB, RARA, FRK, TGM2, MREG, and KRT19. fulvestrant (5 μM), an estrogen receptor (ER) antagonist, was used upon EVI1 knockdown in A2780 cells. Data are presented as means ± S.D. *p < 0.05, **p < 0.01, ***p < 0.001, and ****p < 0.0001.

## 4. Discussion

A high frequency of somatic copy number alterations is a hallmark of HGSOC. The 3q26 amplicon is one of the most amplified chromosomal regions in most human cancers (Bass et al., 2009). EVI1 is located on the 3q26 amplicon which has been reported to be associated with a wide range of human malignancies, including ovarian cancer (Nanjundan et al., 2007; Glass et al., 2013). In this study, we analyzed somatic copy number alterations in a large TCGA cohort (n = 1640) and found that EVI1 was amplified in approximately 30% of HGSOC samples. We subsequently analyzed the correlation between amplification and expression, and the results showed a positive correlation, indicating

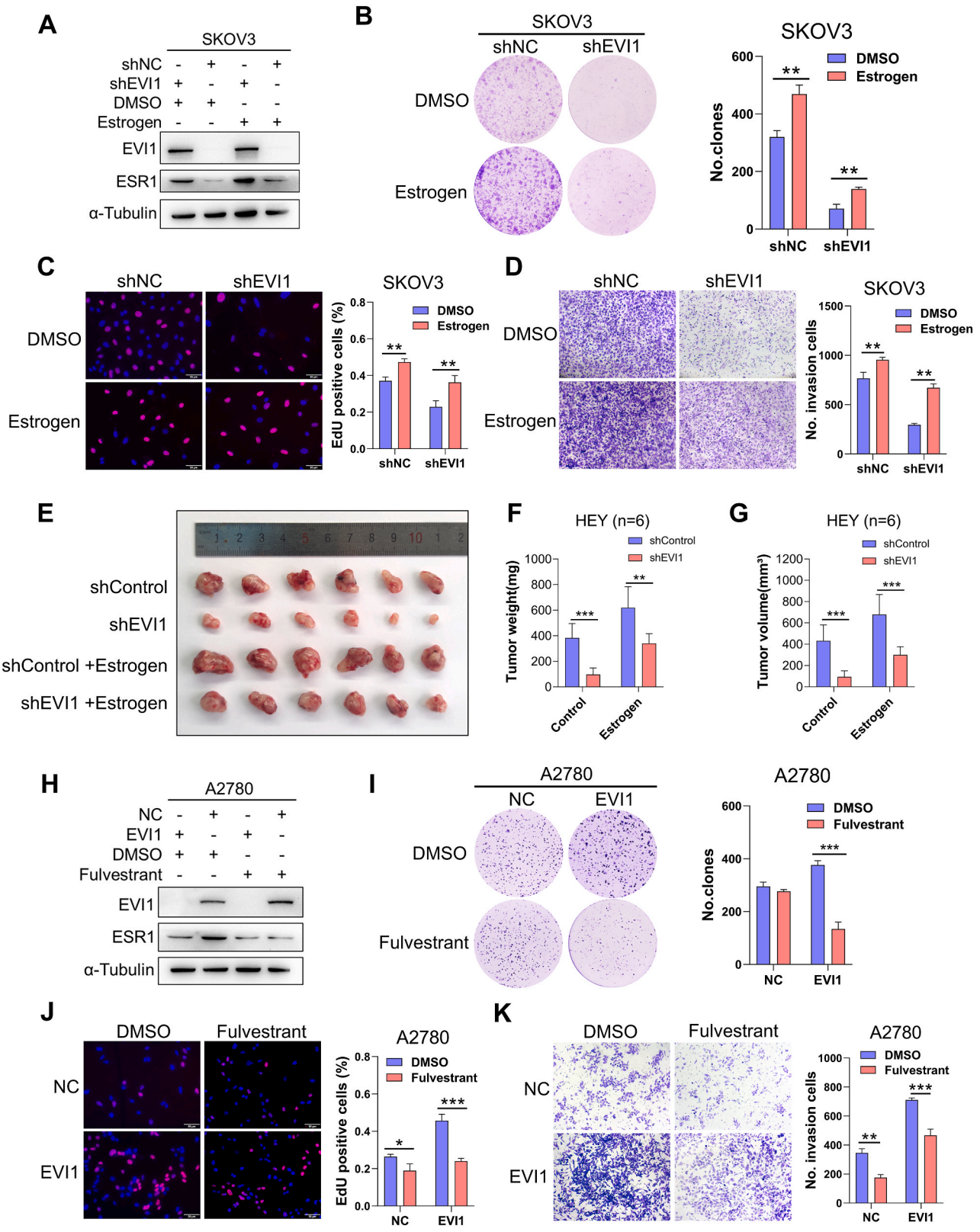


**Fig. 7.** EVI1-induced ESR1 signaling activation is required for ovarian cancer progression. (A) Western blot analysis of ESR1 and EVI1 protein levels in SKOV3 cells treated with estrogen (100 nM). (B-D) Clonogenic, EdU and transwell assays for investigating the potential of estrogen to rescue the loss of EVI1 in SKOV3 cells as indicated (n = 3 biologically independent samples). (E-G) Xenograft model showed estrogen could rescue the loss of EVI1 in tumor growth *in vivo* (n = 6 mice per group). Estradiol benzoate was administered intramuscularly to the xenograft model and DMSO plus phosphate-buffered saline was used as control. The tumor weight and volume were measured for each group. (H) Western blot analysis of ESR1 and EVI1 protein levels in A2780 cells treated with fulvestrant (5 μM). (I-K) Clonogenic, EdU and transwell assays for investigating the potential of fulvestrant to rescue the overexpression of EVI1 in A2780 cells as indicated (n = 3 biologically independent samples). Data are presented as means ± S.D. *p < 0.05, **p < 0.01, ***p < 0.001, and ****p < 0.0001.

higher level of both the EVI1 mRNA and protein in amplification samples than in the diploid group.

The zinc-finger transcription factor EVI1 has been reported to promote malignant progression by regulating the expression of several downstream targets (Mizuguchi et al., 2019; Ma et al., 2019; Ayoub et al., 2018). Here we identified ESR1 as a crucial downstream target of EVI1 in ovarian cancer. EVI1 was enriched at the transcription start site (TSS) region of ESR1 with three clustered TCCTTC binding sites. We then performed ChIP, luciferase assays and CRISPR/Cas9 genome editing to prove that EVI1 directly binds the ESR1 promoter and induces its expression in ovarian cancer cells. We further provided evidence that EVI1 coregulates the ESR1 transcription program and reinforces estrogen signaling. Consistent with the results of our study, the reduced malignant behavior of breast cancer cells caused by EVI1 silencing is rescued by estrogen supplementation (Wang et al., 2017b). In addition to EVI1, FOXA1 and NR2E3 transcriptionally activate ESR1 in breast cancer (Hurtado et al., 2011; Park et al., 2012). In contrast, BRCA1 suppresses ESR1 transcription through the estrogen-responsive enhancer element (Fan et al., 1999). Our observations show for the first time that EVI1 is a key regulator that activates ESR1 expression during the progression of ovarian cancer.

Overexpression of ESR1 has been reported in breast (Hanker et al., 2020), endometrial (Coll-de la Rubia et al., 2020) and ovarian cancers (Zhao et al., 2019). ESR1 expression level is associated with estrogen-dependent growth, invasion and the response to endocrine therapy, particularly in gynecological malignancies (Huang et al., 2014). ESR1 promotes disease progression and participates in drug resistance and metastasis by regulating the PI3K/AKT signaling pathway (Arun et al., 2018; Salmerón-Hernández et al., 2019). In ovarian cancer, ESR1 is dominant and ESR2 replaces estrogen action when ESR1 action is blocked. Interestingly, EVI1 didn't bind to the promoter region of ESR2 in our study, indicating ESR2 was regulated indirectly (Fig. S4C-D).

Endocrine therapy is the most common treatment for ER positive breast cancer (Li et al., 2020). The majority of HGSOC, LGSOC (low grade serous ovarian carcinoma) and endometrioid carcinomas expressing ESR1 respond to endocrine therapy (Langdon et al., 2020). In the present study, we demonstrated that estrogen enhanced the proliferation, invasion and xenograft growth of ovarian cancer cells. Importantly, estrogen could rescue the inhibition of proliferation, invasion and xenograft growth induced by silencing EVI1 (Fig. 7A–G). Consistently, fulvestrant treatment led to a significant reduction in the EVI1-induced proliferation and invasion of A2780 cells (Fig. 7H–K). Resistance to tamoxifen or fulvestrant is a common obstacle, even in patients with ESR1 expression (Piva et al., 2014). However, the molecular mechanism underlying this resistance remain unclear. Our study identified EVI1 as a novel transcription factor that induced ESR1 expression in ovarian cancer and coregulated ESR1 signaling independent of ESR1. Arsenic trioxide (ATO) and PIP1 are small molecule antagonists targeting EVI1 (Bell et al., 2011). ATO has been used to treat acute myeloid leukemia and has been shown to be a potent anticancer agent in various carcinomas (Hoonjan et al., 2018). Strategies targeting EVI1 may be an effective alternative treatment for patients with ER-positive cancer. Further studies are required to determine the therapeutic effect of EVI1 inhibitors on ER-positive cancer.

In conclusion, our study demonstrates that the oncogenic transcription factor EVI1 is frequently amplified and overexpressed in HGSOC. We also provide strong evidence that EVI1 regulates estrogen signaling by directly inducing ESR1 transcription as well as coregulates the ESR1 transcription program and reinforces estrogen signaling. Our findings suggest that EVI1 functions as a novel regulator of the estrogen receptor signaling pathway in ovarian cancer.

## Author contributions statement

Conception and design: BK; ZL; PL. Development and methodology: ZW; YL; XT; SW; NW. Acquisition of data: ZW; YL; XT; SW. Analysis and interpretation of data: ZW; YL; XZ; LZ; NW; ZL. Administrative, technical, or material support: LZ; XZ; ZL; PL. Study supervision: KB; ZL; PL. Writing, review, and/or revision of the manuscript: All authors. Final approval: All authors.

## Declaration of competing interest

The authors declare no conflict of interest.

## Acknowledgements

We thank Translational Medicine Core Facility of Shandong University for consultation and instrument availability that supported this work. This work was supported by National Natural Science Foundation of China (81972437, 81672578, 81902650).

## Appendix A. Supplementary data

Supplementary data to this article can be found online at https://doi.org/10.1016/j.mce.2021.111367.

## References

Arun, A., Ansari, M.I., Popli, P., Jaiswal, S., Mishra, A.K., Dwivedi, A., Hajela, K., Konwar, R., 2018. New piperidine derivative DTPEP acts as dual-acting anti-breast cancer agent by targeting ERα and downregulating PI3K/Akt-PKCα leading to caspase-dependent apoptosis. Cell Prolif 51, e12501.

Ayoub, E., Wilson, M.P., McGrath, K.E., Li, A.J., Frisch, B.J., Palis, J., Calvi, L.M., Zhang, Y., Perkins, A.S., 2018. EVI1 overexpression reprograms hematopoiesis via upregulation of Spi1 transcription. Nat. Commun. 9, 4239.

Bard-Chapeau, E.A., Jeyakani, J., Kok, C.H., Muller, J., Chua, B.Q., Gunaratne, J., Batagov, A., Jenjaroenpun, P., Kuznetsov, V.A., Wei, C.L., D'Andrea, R.J., Bourque, G., Jenkins, N.A., Copeland, N.G., 2012. Ecotopic viral integration site 1 (EVI1) regulates multiple cellular processes important for cancer and is a synergistic partner for FOS protein in invasive tumors. Proc. Natl. Acad. Sci. U. S. A. 109, 2168–2173.

Bass, A.J., Watanabe, H., Mermel, C.H., Yu, S., Perner, S., Verhaak, R.G., Kim, S.Y., Wardwell, L., Tamayo, P., Gat-Viks, I., Ramos, A.H., Woo, M.S., Weir, B.A., Getz, G., Beroukhim, R., O'Kelly, M., Dutt, A., Rozenblatt-Rosen, O., Dziunycz, P., Komisarof, J., Chirieac, L.R., Lafargue, C.J., Scheble, V., Wilbertz, T., Ma, C., Rao, S., Nakagawa, H., Stairs, D.B., Lin, L., Giordano, T.J., Wagner, P., Minna, J.D., Gazdar, A.F., Zhu, C.Q., Brose, M.S., Cecconello, I., Ribeiro Jr., U., Marie, S.K., Dahl, O., Shivdasani, R.A., Tsao, M.S., Rubin, M.A., Wong, K.K., Regev, A., Hahn, W. C., Beer, D.G., Rustgi, A.K., Meyerson, M., 2009. SOX2 is an amplified lineage-survival oncogene in lung and esophageal squamous cell carcinomas. Nat. Genet. 41, 1238–1242.

Bell, D., Berchuck, A., Birrer, M., Chien, J., Cramer, D.W., Dao, F., Dhir, R., DiSaia, P., Gabra, H., Glenn, P., Godwin, A.K., Gross, J., Hartmann, L., Huang, M., Huntsman, D.G., Iacocca, M., Imielinski, M., Kalloger, S., Karlan, B.Y., Levine, D.A., Mills, G.B., Morrison, C., Mutch, D., Olvera, N., Orsulic, S., Park, K., Petrelli, N., Rabeno, B., Rader, J.S., Sikic, B.I., Smith-McCune, K., Sood, A.K., Bowtell, D., Penny, R., Testa, J.R., Chang, K., Creighton, C.J., Dinh, H.H., Drummond, J.A., Fowler, G., Gunaratne, P., Hawes, A.C., Kovar, C.L., Lewis, L.R., Morgan, M.B., Newsham, I.F., Santibanez, J., Reid, J.G., Trevino, L.R., Wu, Y.Q., Wang, M., Muzny, D.M., Wheeler, D.A., Gibbs, R.A., Getz, G., Lawrence, M.S., Cibulskis, K., Sivachenko, A.Y., Sougnez, C., Voet, D., Wilkinson, J., Bloom, T., Ardlie, K., Fennell, T., Baldwin, J., Nichol, R., Fisher, S., Gabriel, S., Lander, E.S., Ding, L., Fulton, R.S., Koboldt, D.C., McLellan, M.D., Wylie, T., Walker, J., O'Laughlin, M., Dooling, D.J., Fulton, L., Abbott, R., Dees, N.D., Zhang, Q., Kandoth, C., Wendl, M., Schierding, W., Shen, D., Harris, C.C., Schmidt, H., Kalicki, J., Delehaunty, K.D., Fronick, C.C., Demeter, R., Cook, L., Wallis, J.W., Lin, L., Magrini, V.J., Hodges, J.S., Eldred, J.M., Smith, S.M., Pohl, C.S., Vandin, F., Upfal, E., Raphael, B.J., Weinstock, G.M., Mardis, E.R., Wilson, R.K., Meyerson, M., Winckler, W., Getz, G., Verhaak, R.G.W., Carter, S.L., Mermel, C.H., Saksena, G., Nguyen, H., Onofrio, R.C., Lawrence, M.S., Hubbard, D., Gupta, S., Crenshaw, A., Ramos, A.H., Ardlie, K., Chin, L., Protopopov, A., Zhang, J., Kim, T.M., Perna, I., Xiao, Y., Zhang, H., Ren, G., Sathiamoorthy, N., Park, R.W., Lee, E., Park, P.J., Kucherlapati, R., Absher, D.M., Waite, L., Sherlock, G., Brooks, J.D., Li, J.Z., Xu, J., Myers, R.M., Laird, P.W., Cope, L., Herman, J.G., Shen, H., Weisenberger, D.J., Noushmehr, H., Pan, F., Triche Jr., T., Berman, B.P., Van Den Berg, D.J., Buckley, J., Baylin, S.B., Spellman, P.T., Purdom, E., Neuvial, P., Bengtsson, H., Jakkula, L.R., Durinck, S., Han, J., Dorton, S., Marr, H., Choi, Y.G., Wang, V., Wang, N.J., Ngai, J., Conboy, J. G., Parvin, B., Feiler, H.S., Speed, T.P., Gray, J.W., Levine, D.A., Socci, N.D., Liang, Y., Taylor, B.S., Schultz, N., Borsu, L., Lash, A.E., Brennan, C., Viale, A., Sander, C., Ladanyi, M., Hoadley, K.A., Meng, S., Du, Y., Shi, Y., Li, L., Turman, Y.J., Zang, D., Helms, E.B., Balu, S., Zhou, X., Wu, J., Topal, M.D., Hayes, D.N., Perou, C. M., Getz, G., Voet, D., Saksena, G., Zhang, J., Zhang, H., Wu, C.J., Shukla, S., Cibulskis, K., Lawrence, M.S., Sivachenko, A., Jing, R., Park, R.W., Liu, Y., Park, P.J.,

Noble, M., Chin, L., Carter, H., Kim, D., Samayoa, J., Karchin, R., Spellman, P.T., Purdom, E., Neuvial, P., Bengtsson, H., Durinck, S., Han, J., Korkola, J.E., Heiser, L. M., Cho, R.J., Hu, Z., Parvin, B., Speed, T.P., Gray, J.W., Schultz, N., Cerami, E., Taylor, B.S., Olshen, A., Reva, B., Antipin, Y., Shen, R., Mankoo, P., Sheridan, R., Ciriello, G., Chang, W.K., Bernanke, J.A., Borsu, L., Levine, D.A., Ladanyi, M., Sander, C., Haussler, D., Benz, C.C., Stuart, J.M., Benz, S.C., Sanborn, J.Z., Vaske, C. J., Zhu, J., Szeto, C., Scott, G.K., Yau, C., Hoadley, K.A., Du, Y., Balu, S., Hayes, D.N., Perou, C.M., Wilkerson, M.D., Zhang, N., Akbani, R., Baggerly, K.A., Yung, W.K., Mills, G.B., Weinstein, J.N., Penny, R., Shelton, T., Grimm, D., Hatfield, M., Morris, S., Yena, P., Rhodes, P., Sherman, M., Paulauskis, J., Millis, S., Kahn, A., Greene, J.M., The Cancer Genome Atlas Research, N., Disease working, g., tissue source, s., Genome sequencing centres Baylor College of, M., Broad, I., Washington University in St, L., Cancer genome characterization centres Broad Institute/Dana-Farber Cancer, I., Harvard Medical, S., HudsonAlpha Institute/Stanford, U., University of Southern California/Johns Hopkins, U., Lawrence Berkeley National, L., Memorial Sloan-Kettering Cancer, C., University of North Carolina at Chapel, H., Genome data analysis centres Broad, I., Johns Hopkins, U., University of California Santa Cruz/Buck, I., The University of Texas, M.D.A.C.C., Biospecimen core, r., Data coordination, c., 2011. Integrated genomic analyses of ovarian carcinoma. Nature 474, 609–615.

Coll-de la Rubia, E., Martinez-Garcia, E., Dittmar, G., Gil-Moreno, A., Cabrera, S., Colas, E., 2020. Prognostic biomarkers in endometrial cancer: a systematic review and meta-analysis. J. Clin. Med. 9.

Fan, S., Wang, J., Yuan, R., Ma, Y., Meng, Q., Erdos, M.R., Pestell, R.G., Yuan, F., Auborn, K.J., Goldberg, I.D., Rosen, E.M., 1999. BRCA1 inhibition of estrogen receptor signaling in transfected cells. Science 284, 1354–1356.

Fears, S., Mathieu, C., Zeleznik-Le, N., Huang, S., Rowley, J.D., Nucifora, G., 1996. Intergenic splicing of MDS1 and EVI1 occurs in normal tissues as well as in myeloid leukemia and produces a new member of the PR domain family. Proc. Natl. Acad. Sci. U.S.A. 93, 1642–1647.

Feng, J.X., Liu, T., Qin, B., Zhang, Y., Liu, X.S., 2012. Identifying ChIP-seq enrichment using MACS. Nat. Protoc. 7, 1728–1740.

Funabiki, T., Kreider, B.L., Ihle, J.N., 1994. The carboxyl domain of zinc fingers of the Evi-1 myeloid transforming gene binds a consensus sequence of GAAGATGAG. Oncogene 9, 1575–1581.

Glass, C., Wuertzer, C., Cui, X., Bi, Y., Davuluri, R., Xiao, Y.Y., Wilson, M., Owens, K., Zhang, Y., Perkins, A., 2013. Global identification of EVI1 target genes in acute myeloid leukemia. PloS One 8, e67134.

Goldman, M.J., Craft, B., Hastie, M., Repecka, K., McDade, F., Kamath, A., Banerjee, A., Luo, Y., Rogers, D., Brooks, A.N., Zhu, J., Haussler, D., 2020. Visualizing and interpreting cancer genomics data via the Xena platform. Nat. Biotechnol. 38, 675–678.

Hanker, A.B., Sudhan, D.R., Arteaga, C.L., 2020. Overcoming endocrine resistance in breast cancer. Canc. Cell 37, 496–513.

Hoonjan, M., Jadhav, V., Bhatt, P., 2018. Arsenic trioxide: insights into its evolution to an anticancer agent. J. Biol. Inorg. Chem. 23, 313–329.

Huang, B., Omoto, Y., Iwase, H., Yamashita, H., Toyama, T., Coombes, R.C., Filipovic, A., Warner, M., Gustafsson, J.-Å., 2014. Differential expression of estrogen receptor α, β1, and β2 in lobular and ductal breast cancer, 111, 1933–1938.

Hurtado, A., Holmes, K.A., Ross-Innes, C.S., Schmidt, D., Carroll, J.S., 2011. FOXA1 is a key determinant of estrogen receptor function and endocrine response. Nat. Genet. 43, 27–33.

Idel, C., Ribbat-Idel, J., Kuppler, P., Krupar, R., Offermann, A., Vogel, W., Rades, D., Kirfel, J., Wollenberg, B., Perner, S., 2020. EVI1 as a marker for lymph node metastasis in HNSCC. Int. J. Mol. Sci. 21.

Jazaeri, A.A., Ferriss, J.S., Bryant, J.L., Dalton, M.S., Dutta, A., 2010. Evaluation of EVI1 and EVI1s (Δ324) as potential therapeutic targets in ovarian cancer. Gynecol. Oncol. 118, 189–195.

Labidi-Galy, S.I., Papp, E., Hallberg, D., Niknafs, N., Adleff, V., Noe, M., Bhattacharya, R., Novak, M., Jones, S., Phallen, J., Hruban, C.A., Hirsch, M.S., Lin, D.I., Schwartz, L., Maire, C.L., Tille, J.-C., Bowden, M., Ayhan, A., Wood, L.D., Scharpf, R.B., Kurman, R., Wang, T.-L., Shih, I.-M., Karchin, R., Drapkin, R., Velculescu, V.E., 2017. High grade serous ovarian carcinomas originate in the fallopian tube. Nat. Commun. 8, 1093.

Langdon, S.P., Herrington, C.S., Hollis, R.L., Gourley, C., 2020. Estrogen signaling and its potential as a target for therapy in ovarian cancer. Cancers 12.

Li, L., Lin, L., Veeraraghavan, J., Hu, Y., Wang, X., Lee, S., Tan, Y., Schiff, R., Wang, X.S., 2020. Therapeutic role of recurrent ESR1-CCDC170 gene fusions in breast cancer endocrine resistance. Breast Cancer Res. 22, 84.

Liberzon, A., Birger, C., Thorvaldsdóttir, H., Ghandi, M., Jill, Mesirov, P., Tamayo, P., 2015. The molecular signatures database hallmark gene set collection. Cell Systems 1, 417–425.

Lugthart, S., van Drunen, E., van Norden, Y., van Hoven, A., Erpelinck, C.A.J., Valk, P.J. M., Beverloo, H.B., Löwenberg, B., Delwel, R., 2008. High EVI1 levels predict adverse outcome in acute myeloid leukemia: prevalence of EVI1 overexpression and chromosome 3q26 abnormalities underestimated. Blood 111, 4329–4337.

Ma, H., Li, Y., Wang, X., Wu, H., Qi, G., Li, R., Yang, N., Gao, M., Yan, S., Yuan, C., Kong, B., 2019. PBK, targeted by EVI1, promotes metastasis and confers cisplatin resistance through inducing autophagy in high-grade serous ovarian carcinoma. Cell Death Dis. 10, 166.

Mi, H., Ebert, D., Muruganujan, A., Mills, C., Albou, L.P., Mushayamaha, T., Thomas, P. D., 2020. PANTHER version 16: a revised family classification, tree-based classification tool, enhancer regions and extensive API. Nucleic Acids Res. 49, D394–D403.

Mizuguchi, A., Yamashita, S., Yokogami, K., Morishita, K., Takeshima, H., 2019. Ecotropic viral integration site 1 regulates EGFR transcription in glioblastoma cells. J. Neuro Oncol. 145, 223–231.

Nanjundan, M., Nakayama, Y., Cheng, K.W., Lahad, J., Liu, J., Lu, K., Kuo, W.L., Smith-McCune, K., Fishman, D., Gray, J.W., Mills, G.B., 2007. Amplification of MDS1/EVI1 and EVI1, located in the 3q26.2 amplicon, is associated with favorable patient prognosis in ovarian cancer. Canc. Res. 67, 3074–3084.

Nucifora, G., 1997. The EVI1 gene in myeloid leukemia. Leukemia 11, 2022–2031.

Park, Y.Y., Kim, K., Kim, S.B., Hennessy, B.T., Kim, S.M., Park, E.S., Lim, J.Y., Li, J., Lu, Y., Gonzalez-Angulo, A.M., Jeong, W., Mills, G.B., Safe, S., Lee, J.S., 2012. Reconstruction of nuclear receptor network reveals that NR2E3 is a novel upstream regulator of ESR1 in breast cancer. EMBO Mol. Med. 4, 52–67.

Piva, M., Domenici, G., Iriondo, O., Rabano, M., Simoes, B.M., Comaills, V., Barredo, I., Lopez-Ruiz, J.A., Zabalza, I., Kypta, R., Vivanco, M., 2014. Sox2 promotes tamoxifen resistance in breast cancer cells. EMBO Mol. Med. 6, 66–79.

Pradhan, A.K., Mohapatra, A.D., Nayak, K.B., Chakraborty, S., 2011. Acetylation of the proto-oncogene EVI1 abrogates Bcl-xL promoter binding and induces apoptosis. PloS One 6, e25370.

Quinlan, A.R., Hall, I.M., 2010. BEDTools: a flexible suite of utilities for comparing genomic features. Bioinformatics 26, 841–842.

Ran, F.A., Hsu, P.D., Wright, J., Agarwala, V., Scott, D.A., Zhang, F., 2013. Genome engineering using the CRISPR-Cas9 system. Nat. Protoc. 8, 2281–2308.

Ritchie, M.E., Phipson, B., Wu, D., Hu, Y., Law, C.W., Shi, W., Smyth, G.K., 2015. Limma powers differential expression analyses for RNA-sequencing and microarray studies. Nucleic Acids Res. 43, e47.

Robinson, J.T., Thorvaldsdóttir, H., Wenger, A.M., Zehir, A., Mesirov, J.P., 2017. Variant Review with the Integrative Genomics Viewer, 77, pp. e31–e34.

Ross-Innes, C.S., Stark, R., Teschendorff, A.E., Holmes, K.A., Ali, H.R., Dunning, M.J., Brown, G.D., Gojis, O., Ellis, I.O., Green, A.R., Ali, S., Chin, S.-F., Palmieri, C., Caldas, C., Carroll, J.S., 2012. Differential oestrogen receptor binding is associated with clinical outcome in breast cancer. Nature 481, 389–393.

Salmerón-Hernández, Á., Noriega-Reyes, M.Y., Jordan, A., Baranda-Avila, N., Langley, E., 2019. BCAS2 enhances carcinogenic effects of estrogen receptor alpha in breast cancer cells. Int. J. Mol. Sci. 20.

Shimabe, M., Goyama, S., Watanabe-Okochi, N., Yoshimi, A., Ichikawa, M., Imai, Y., Kurokawa, M., 2009. Pbx1 is a downstream target of Evi-1 in hematopoietic stem/progenitors and leukemic cells. Oncogene 28, 4364–4374.

Siegel, R.L., Miller, K.D., Jemal, A., 2019. Cancer statistics, 2019. CA: A Canc. J. Clinic. 69, 7–34.

Subramanian, A., Tamayo, P., Mootha, V.K., Mukherjee, S., Ebert, B.L., Gillette, M.A., Paulovich, A., Pomeroy, S.L., Golub, T.R., Lander, E.S., Mesirov, J.P., 2005. Gene set enrichment analysis: A knowledge-based approach for interpreting genome-wide expression profiles, 102, 15545–15550.

Tanaka, T., Nishida, J., Mitani, K., Ogawa, S., Yazaki, Y., Hirai, H., 1994. Evi-1 raises AP-1 activity and stimulates c-fos promoter transactivation with dependence on the second zinc finger domain. J. Biol. Chem. 269, 24020–24026.

Tang, Z., Kang, B., Li, C., Chen, T., Zhang, Z., 2019. GEPIA2: an enhanced web server for large-scale expression profiling and interactive analysis. Nucleic Acids Res. 47, W556–W560.

Wang, Y., Zhang, X., Tang, W., Lin, Z., Xu, L., Dong, R., Li, Y., Li, J., Zhang, Z., Li, X., Zhao, L., Wei, J.-J., Shao, C., Kong, B., Liu, Z., 2017a. miR-130a upregulates mTOR pathway by targeting TSC1 and is transactivated by NF-κB in high-grade serous ovarian carcinoma. Cell Death Differ. 24, 2089–2100.

The, C., 2019. Gene Ontology, the gene Ontology resource: 20 years and still GOing strong. Nucleic Acids Res. 47, D330–D338.

Wang, H., Schaefer, T., Konantz, M., Braun, M., Varga, Z., Paczulla, A.M., Reich, S., Jacob, F., Perner, S., Moch, H., Fehm, T.N., Kanz, L., Schulze-Osthoff, K., Lengerke, C., 2017b. Prominent oncogenic roles of EVI1 in breast carcinoma. Canc. Res. 77, 2148–2160.

Yu, G., Wang, L.-G., He, Q.-Y., 2015. ChIPseeker: an R/Bioconductor package for ChIP peak annotation, comparison and visualization. Bioinformatics 31, 2382–2383.

Yuasa, H., Oike, Y., Iwama, A., Nishikata, I., Sugiyama, D., Perkins, A., Mucenski, M.L., Suda, T., Morishita, K., 2005. Oncogenic transcription factor Evi1 regulates hematopoietic stem cell proliferation through GATA-2 expression. EMBO J. 24, 1976–1987.

Zhang, S., Li, X., Burghardt, R., Smith, R., Safe, S.H., 2005. Role of estrogen receptor (ER) α in insulin-like growth factor (IGF)-I-induced responses in MCF-7 breast cancer cells. J. Mol. Endocrinol. 35, 433–447.

Zhao, S.G., Chen, W.S., Das, R., Chang, S.L., Tomlins, S.A., Chou, J., Quigley, D.A., Dang, H.X., Barnard, T.J., Mahal, B.A., Gibb, E.A., Liu, Y., Davicioni, E., Duska, L.R., Posadas, E.M., Jolly, S., Spratt, D.E., Nguyen, P.L., Maher, C.A., Small, E.J., Feng, F. Y., 2019. Clinical and genomic implications of luminal and basal subtypes across carcinomas. Clin. Canc. Res. 25, 2450–2457.